Extended Abstracts of the 2002 International Conference on Solid State Devices and Materials, Nagoya, 2002, pp. 418-419

LP2-2

Physical RF modeling of Junction Varactors

Youngjoon Ahn, Kwangsuk Han, and Hyungcheol Shin
Department of Electrical Engineering and Computer Science, KAIST
373-1, Guseong-dong, Yuseong-gu, Daejeon, 305-701, Korea
Phone: +82-42-869-5459 Fax: +82-42-869-8590 E-mail: nanom@inca.kaist.ac.kr

1. Introduction

Of the CMOS-based RFIC components, junction varactors can be used in the LC tank of VCO [1,2]. The capacitance tuning range of the junction varactors affects the frequency tuning range of the VCO and the quality factor of the varactors influences phase noise [3]. So, an accurate model of junction varactor is needed in order to correctly predict the VCO characteristics.

In this paper, a physical model, which is accurate and scalable over a wide range of layout dimensions, is proposed and the simulation results of this model have been compared with the measurement data.

2. Proposed Model and Modeling Results

p^+/n-well junction varactors with different device geometries were fabricated using 0.25μm CMOS technology. The size of the finger was fixed as L=0.58μm, W=50μm and the number of fingers was varied with N=6, 12, 24. Two-port S-parameter measurement was performed for the frequency range of 0.5GHz to 20GHz. The parasitic effects of the probe pads were de-embedded with open and short test patterns.

Fig. 1 shows the cross-section of the p^+/n-well junction varactor. Fig. 2 shows RF model based on physical structure. C_{jc} is the junction capacitance between the p^+ region and n-well region. R_D is the n-well region resistance between depletion region and n^+ region. R_{well} is the n-well region resistance toward substrate, C_{sub1} is the capacitance between the n-well and p-substrate, and R_{sub} and C_{sub2} model the parasitic effect due to the substrate. The equivalent circuit model using RF model shown in Fig. 2 is shown in Fig. 3. In this equivalent circuit, C_p represents ground proximity effect and L is the series inductance caused by metal line on the p^+/n^+ diffusion.

The values of parameters in the equivalent circuit can be extracted from y-parameters. Y_{12} can be expressed as follows;

$$-\frac{1}{Y_{12}} = R_D + j\left(\omega L - \frac{1}{\omega C_{jc}}\right) \quad (1)$$

R_D was directly extracted from Re $[-1/Y_{12}]$ (Fig. 4). L and C_{jc} were determined from the slope and -1/(y-intercept point) in the plot of $\omega \times$ Im $[-1/Y_{12}]$ versus ω^2 (Fig. 5).

$$\omega \times \mathrm{Im}\left[-\frac{1}{Y_{12}}\right] = \omega^2 L - \frac{1}{C_{jc}} \quad (2)$$

R_{sub}, R_{well}, C_{sub1} and C_{sub2} can be extracted from $(Y_{12}+Y_{22})$ using the following relationship.

$$\frac{1}{Y_{12}+Y_{22}} = R_{well} + \frac{R_{sub}}{1+\omega^2 R_{sub}^2 C_{sub2}^2} - j\left(\frac{1}{\omega C_{sub1}} + \frac{\omega R_{sub}^2 C_{sub2}}{1+\omega^2 R_{sub}^2 C_{sub2}^2}\right) \quad (3)$$

Assuming $\omega^2 R_{sub}^2 C_{sub2}^2 \ll 1$ at low frequency, the real part of Eq. (3) can be expressed as Eq. (4) (Fig. 6).

$$\mathrm{Re}\left[\frac{1}{Y_{12}+Y_{22}}\right] = R_{well} + R_{sub} = \mathrm{K} \quad (4)$$

Replacing R_{well} in the real part of Eq. (3) with $(K-R_{sub})$, It can be expressed as follows;

$$-\frac{1}{\mathrm{Re}[1/(Y_{12}+Y_{22})]-\mathrm{K}} = \frac{1}{R_{sub}} + \frac{1}{\omega^2 R_{sub}^3 C_{sub2}^2} \quad (5)$$

R_{sub} and C_{sub2} can be determined from the y-intercept point and the slope in the plot of -1/(Re $[1/(Y_{12}+Y_{22})]$-K) versus $1/\omega^2$ (Fig. 7). And R_{well} can be obtained by using Eq. (4).

Also, assuming $\omega^2 R_{sub}^2 C_{sub2}^2 \ll 1$ at low frequency and multiplying each term by ω, the imaginary part of Eq. (3) is expressed as

$$-\omega \times \mathrm{Im}\left[\frac{1}{Y_{12}+Y_{22}}\right] = \frac{1}{C_{sub1}} + \omega^2 R_{sub}^2 C_{sub2} \quad (6)$$

Here, C_{sub1} can be obtained using the y-intercept point in the plot of $-\omega \times$ Im $[1/(Y_{12}+Y_{22})]$ versus ω^2 (Fig. 8). Finally, C_P can be directly extracted from Im $[Y_{11}+Y_{12}] / \omega$ (Fig. 9). At 3GHz, $\omega^2 R_{sub}^2 C_{sub2}^2$ was calculated to be 0.08, therefore the assumption of $\omega^2 R_{sub}^2 C_{sub2}^2 \ll 1$ is valid.

After direct extraction, the values were optimized further. By using optimized parameter value, the scaling rules, which have physical meaning, are determined to describe the behavior of junction varactor with various device geometries.

Fig. 10 shows the measured and modeled C_{jc} of three devices with Vr (reverse bias). This shows that the proposed scaling rule, which results from the physical equivalent circuit and therefore has physical meaning, can be applied to various bias range and various device sizes.

Fig. 11 shows the measured and modeled Q factors. The good agreements between the measurement and model make it easy to design RFIC with this model.

Fig. 12 shows that there is excellent agreement between the measured and modeled s-parameters of device (N=24) at Vr = 0V.

The mean error of each device was less than 3.5%.

4. Conclusions

A scalable junction varactor model for RF has been developed in this paper. The model composed of physical components is valid up to 20GHz. The model has very high accuracy with mean error less than 3.5 %.

References

[1] A.S. Porret, et al., IEEE JSSC, vol.35, pp.337-345
[2] P. Andreani, et al., IEEE JSSC, vol.35, pp.905-910
[3] Maget. J, et al. ISDRS, pp. 609-612

Acknowledgement

This work was supported by the KOSEF through the MICROS center at KAIST and the Dongbu Electronics Co., Ltd.

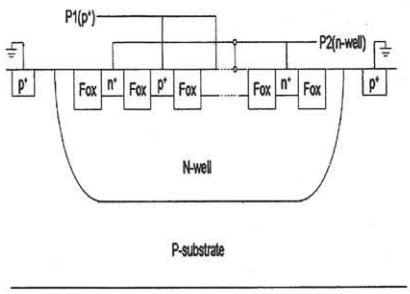

Fig. 1 The cross-section of junction varactor.

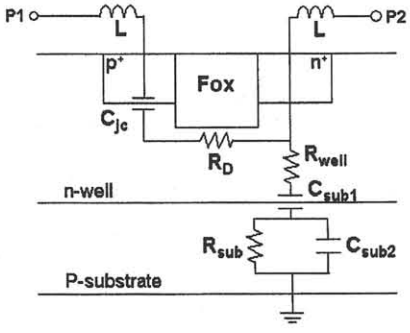

Fig. 2 The RF junction varactor model based on physical structure.

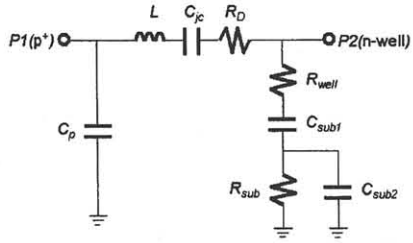

Fig. 3 The equivalent circuit of junction varactor.

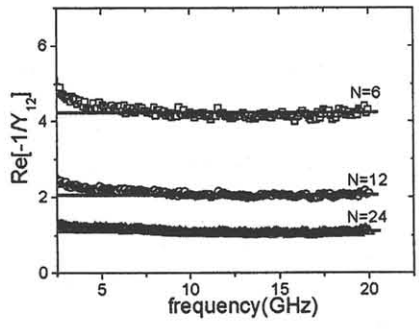

Fig. 4. The plot of Re $[-1/Y_{12}]$ versus frequency at Vr = 1.8V for three devices

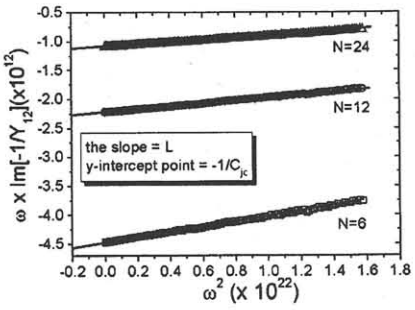

Fig. 5 The plot of $\omega \times \text{Im}\,[-1/Y_{12}]$ versus ω^2 at Vr = 1.8V for three devices.

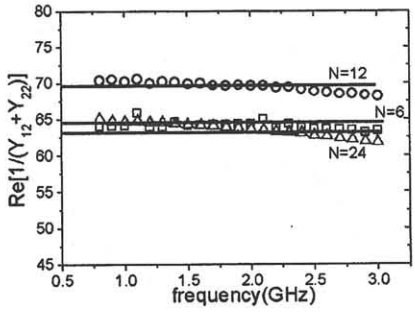

Fig. 6 The plot of Re $[1/(Y_{12}+Y_{22})]$ versus ω at Vr = 1.8V for three devices.

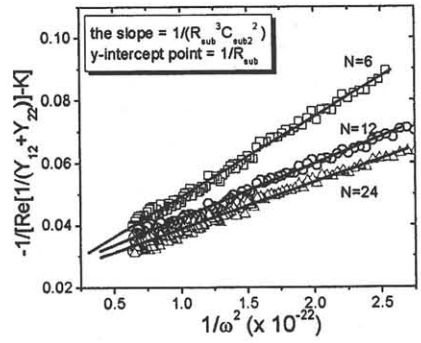

Fig. 7 The plot of -1/[Re $[(1/Y_{12}+Y_{22})]$-K] versus $1/\omega^2$ at Vr = 1.8V for three devices.

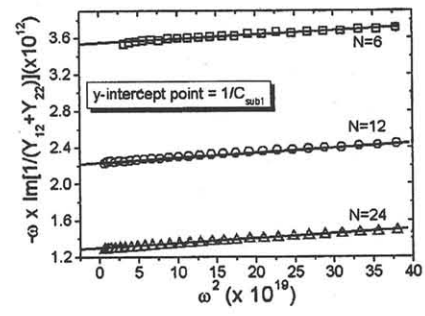

Fig. 8 The plot of $-\omega \times \text{Im}\,[1/(Y_{12}+Y_{22})]$ versus ω^2 at Vr = 1.8V for three devices.

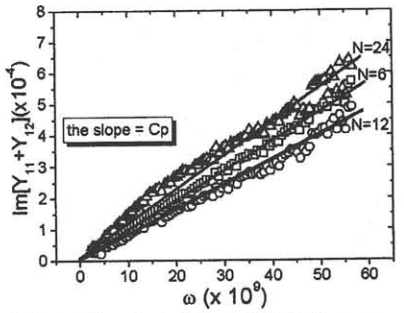

Fig. 9 The plot of Im $[Y_{11}+Y_{12}]$ versus ω at Vr = 1.8 V for three devices.

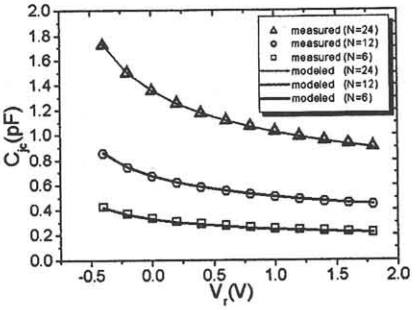

$$C_{jc}(\text{fF}) = \frac{56.878 \times N - 9.14}{(1+\frac{V_r}{0.784})^{0.342}}$$

N = the number of fingers
Vr = reverse bias

Fig. 10. The measured and modeled C_{jc} as a function of varying Vr.

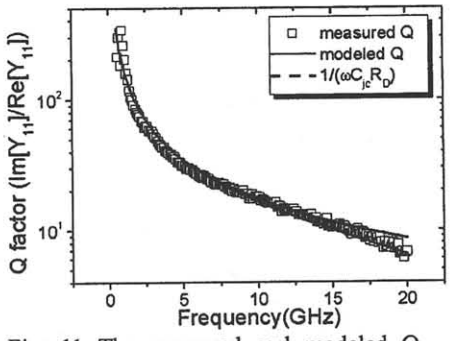

Fig. 11 The measured and modeled Q factors for device which has 24 fingers.

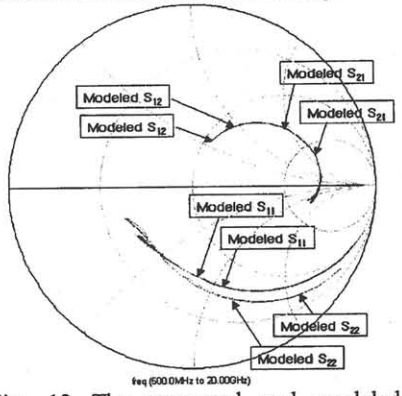

Fig. 12 The measured and modeled S-parameters for device which has 24 fingers.